Effect of transition metal doping on multiferroic ordering in FeVO_{4}

A. Kumarasiri, E. Abdelhamid, A. Dixit, and G. Lawes

Phys. Rev. B **91**, 014420 — Published 15 January 2015

DOI: 10.1103/PhysRevB.91.014420

Effect of transition metal doping on multiferroic ordering in $FeVO_4$

A. Kumarasiri[1*], E. Abdelhamid[1], A. Dixit[1,2], and G. Lawes[1]

1. Department of Physics and Astronomy, Wayne State University, Detroit, MI 48201

2. Center for Energy, Indian Institute of Technology, Jodhpur, India, 342011

*Current address: Henry Ford Health System, Detroit, MI 48202

Abstract

$FeVO_4$ is a multiferroic that undergoes two antiferromagnetic transitions at T_{N1}~21 K and T_{N2}~15 K, with a small ferroelectric polarization developing at the 15 K transition. We have studied the effect of magnetic and non-magnetic transition metal dopants on these magnetic phase transitions in order to investigate the microscopic mechanisms for magnetoelectric coupling in this system as well as probing the evolution of the phase transitions. We have synthesized polycrystalline $Fe_{1-x}TM_xVO_4$(TM = Zn, Cr, Mn) samples up to x=0.2 and studied dynamics of these two ferroic phase transitions using thermodynamic, magnetic, and pyrocurrent measurements. We find that the magnetic ordering temperatures in $FeVO_4$ are remarkably stable, showing only a minimal suppression in transition temperatures even for larger doping fractions. We also observe clear reversible polarization at x=0.05 for all samples, which also persists to the largest doping for Zn, suggesting the multiferroic order persists over a large range of compositions.

PACS: 75.85.+t, 75.30.Kz, 61.72.U-

Multiferroic materials exhibiting simultaneous ferroelectric and ferromagnetic behavior have been a topic of great interest because of their potential applications for functional devices such as magnetic storage media and spintronics[1,2]. Although a relatively large number of multiferroic materials have been discovered and studied in recent years[3,4,5], there remains a number of open questions concerning the origin of the magnetoelectric coupling, particularly in systems exhibiting a magnetically-induced ferroelectric polarization. In order to elucidate the microscopic origins of the magnetoelectric coupling in these systems, there have been a number of investigations on the response of various multiferroic materials under different types of perturbations[6,7,8,9]. Within this broad field of study, chemical doping has been used effectively as a tool to study how the structural, magnetic, and electrical properties of multiferroics are affected by small changes in composition[10,11,12]. Doping studies have also been used to explore how the multiferroic ordering temperature changes and microscopic magnetic interactions that give rise to the multiferroic behavior are affected under perturbations, providing insight into the stability of the magnetic interactions[12,13,14,15].

Previous doping studies on another vanadate multiferroic, $Ni_3V_2O_8$, found a suppression of the magnetic transition temperatures that could be quantitatively explained in terms of magnetic percolation[13,14]. On doping with non-magnetic Zn at Ni site, the suppression of the two magnetic transitions were both consistent with simple site dilution for the corresponding magnetic structure[13]. However, on doping with spin-1/2 Cu at Ni site, the multiferroic ordering was completely suppressed by only 8 at% doping, while on doping with spin-3/2 Co, the multiferroic ordering persisted beyond 30 at% doping[14]. Doping studies on different multiferroics also reveal a range of different behaviors for the transition temperatures, varying from a reduction that is consistent with simple dilution to complete suppression of the multiferroic state for small impurity concentrations. A study on $Ni_3V_2O_8$ and $Co_3V_2O_8$ by Zhang *et al* also finds that Co doping on $Ni_3V_2O_8$ at Ni site only minimally affects the multiferroic order even at high doping fractions, while Ni doping at Co site strongly modulates the magnetic ordering in $Co_3V_2O_8$ even at low compositions[15]. A study on Lanthanum doped multiferroic $DyFeO_3$[12] finds a small

suppression of the antiferromagnetic ordering temperature (T_N) while the spin reorientation phase transition temperature shows a larger suppression.

Studies on multiferroic $MnWO_4$ have indicated that the effects of doping depend strongly on the magnetic properties of the dopant. When non-magnetic Zn and Mg replaced some of the magnetic Mn^{2+} ions, the Neel transition and multiferroic transition temperatures were suppressed linearly with doping fraction[16]. A related study also found that the multiferroic phase of $MnWO_4$ is relatively stable against doping by non-magnetic ions, which persists up to a 50% Zn fraction[17]. However, magnetic dopants were found to strongly suppress the multiferroic ordering on $MnWO_4$. One such study determined that the multiferroic phase of $MnWO_4$ is completely absent at an Fe fraction of only x=0.05[18]. However, doping with Co seems to have a smaller effect on the multiferroic phase transition. A study done on $Mn_{0.85}Co_{0.15}WO_4$ single crystals finds the material is still ferroelectric even at 15% Co doping[19].

In this work, we explore the effects of both non-magnetic (Zn) and magnetic (Cr and Mn) dopants on the multiferroic properties of $FeVO_4$[20], which has significant magnetoelectric coupling[21,22]. $FeVO_4$ is a strongly frustrated system[23], having a Curie-Weiss interaction temperature of 125 K, roughly a factor of six larger than the magnetic ordering temperature[20,21]. $FeVO_4$ undergoes two successive antiferromagnetic transitions at low temperatures; it orders magnetically at a Neel temperature T_{N1} of 21 K where it forms a collinear incommensurate structure, and at T_{N2}~15 K it undergoes a second antiferromagnetic transition to a non-collinear incommensurate structure[20], although it is worth noting that recent studies on single crystal $FeVO_4$ have reported lower transition temperatures; T_{N1}=19 K and T_{N2}=13 K[23], with respect to the previously reported values[20,21,22]. The T_{N2} ~15 K transition is also ferroelectric[20,21], with finite spontaneous electrical polarization developing in this spiral incommensurate magnetic phase. $FeVO_4$ belongs to $P\bar{1}$ space group and is a low symmetry crystal, with three different unique Fe^{3+} lattice sites in the magnetic lattice[20]. Because of the low symmetry in $FeVO_4$, the direction of the polarization is not determined simply from the magnetic structure, but also depends on details of the microscopic magnetoelectric interaction[22]. By replacing

Fe^{3+}(s=5/2) ions with Zn^{2+}(s=0), Cr^{3+}(s=3/2), and Mn^{3+}(s=2), we explore the stability of the magnetic phase transition of $FeVO_4$ against perturbations.

We prepared polycrystalline $Fe_{1-x}TM_xVO_4$ samples over the composition range of x=0 to x=0.2 using a standard solid state reaction method. The parent compound was prepared using V_2O_5 and Fe_2O_3 precursors, with the dopants incorporated by adding suitable oxide or nitrate powders at the appropriate atomic fractions. The mixture was then annealed at 550 ^oC with intermediate grindings to improve homogeneity, and finally annealed at 700 ^oC for an additional 4 hours. The resultant powder was ground and cold pressed into pellets as required for specific measurements. The zinc, chromium and manganese atomic fractions in each of the samples were verified by energy dispersive x-ray spectroscopy (EDS) on a JEOL JSM 6510LV scanning electron microscope equipped with an EDAX spectrometer. These were found to be in good agreement with the expected values, with no other impurities present. The composition as measured by EDS was used to determine the actual dopant fraction.

To probe the crystal structure, we carried out room temperature x-ray diffraction (XRD) studies using a Rigaku RU2000 rotating anode diffractometer. Figures 1 (a), (b) and (c) show the x-ray spectra obtained for $FeVO_4$ doped with different fractions of Zn, Cr, and Mn respectively, plotted together with undoped $FeVO_4$. The curves have been shifted vertically for clarity. We find that all peaks observed in pure $FeVO_4$ are present in the doped samples, with no additional peaks. This implies that there are no substantial crystalline impurity phases in these samples. Because $FeVO_4$ has very low symmetry, it was challenging to fit these low resolution x-ray diffraction data using Reitveld refinement. However, the relative intensity of certain peaks, including the $2\theta = 25.01^o$, $2\theta = 27.67^o$, and $2\theta = 42.05^o$ peaks, did show some changes on changing the dopant concentration. Because XRD is insensitive to small amounts of secondary phases as well as amorphous impurities, we also carried out Raman spectroscopic studies to confirm the phase-purity of these samples.

Figures 2 (a), (b) and (c) show the room temperature Raman spectra collected for $FeVO_4$ doped with Zn, Cr and Mn respectively at different dopant concentrations. The curves have been shifted vertically for clarity. We observe 17 main Raman modes in undoped $FeVO_4$, which are all present in the spectra for the doped samples as well. The absence of any other peaks in these spectra strongly suggests that the doped samples have the correct $FeVO_4$ structure with no additional impurity phases. The Raman modes at 733, 842, and 928 cm^{-1},which are associated with the stretching of Fe–O and V–O–Fe bonds and the bending of Fe–O–V and Fe–O–Fe complexes[21], are suppressed to lower wave numbers with increasing Zn fraction (Fig 2 (a)). This is consistent with the expected shift in the vibrational frequencies as higher mass Zn atoms (65.4 amu) replace some of the lighter Fe ions (55.8 amu). There is no clear shift in the Raman spectra for the Cr (52 amu) and Mn (54.9 amu) dopants because the mass difference relative to Fe is much smaller. These results, together with small changes in relative peak intensities observed in the XRD data, are consistent with the dopant transition metal ions replacing Fe^{3+} ions in the lattice. Fe^{3+} has an ionic radius of 0.55 pm in this coordination, while Cr^{3+} and Mn^{3+} have radii of 0.49 pm and 0.58 pm respectively[24], so these dopants should fit readily into the lattice. Zn^{2+} is slightly larger, having a radius of 0.74 pm, but is apparently still able to fit into the $FeVO_4$ lattice up to a doping fraction of x=0.20.

We used magnetic measurements to both identify the onset of the antiferromagnetic phase transitions at low temperatures and to estimate the effective moments and interactions in the paramagnetic regime at higher temperatures. The magnetization as a function of temperature from 5 K to 300 K for the Zn doped samples is plotted in Fig. 3 (a), with the insert showing the low temperature behavior. The high temperature magnetization data was used to fit the Curie-Weiss function (as shown in Fig. 4), to estimate the Curie-Weiss temperature and magnetic contribution for these samples. The anomalies associated with antiferromagnetic transitions for $Fe_{1-x}TM_xVO_4$ [TM = Zn, Cr, Mn] samples can be clearly observed in the lower temperature magnetization versus temperature data, as explained in Fig. 3(a), (b) and (c) respectively. There is some additional paramagnetic signal that emerges at very low temperatures in the doped samples, particularly the x=0.20 sample, which we attribute to orphan spins[25,26]. In all

cases, the antiferromagnetic ordering temperature at T_{N1}~21 K is clearly indicated by a sharp peak, while the second antiferromagnetic transition, marking the onset of multiferroic order, T_{N2}~15 K, is only seen as a small change in slope of the magnetization. These results are consistent with previously observed magnetization curves for undoped $FeVO_4$[20,21]. These data confirm that both magnetic transitions in $FeVO_4$ persist even with 20% doping of Zn, Cr and Mn, and show only a minimal suppression of the transition temperature.

In order to further characterize the magnetic properties of these samples, we plot the inverse magnetization against temperature for the x=0.05 and x=0.20 $Fe_{1-x}TM_xVO_4$ samples in Figs 4 (a) and 4 (b), respectively. The paramagnetic response of these samples was modeled using the Curie Weiss law $\chi = C/(T - T_\theta)$, where $C = Ng^2\mu_B^2J(J + 1)/3k_B$ is the Curie constant and T_θ the Curie-Weiss temperature to estimate the effective magnetic moment and Curie-Weiss temperature. We find the effective moments, per transition metal ion, to be 5.81 μ_B, 5.82 μ_B, and 5.85 μ_B at x=0.05, and 5.44 μ_B, 5.5 μ_B, and 5.63 μ_B at x=0.20 for $FeVO_4$ doped with Zn, Cr, and Mn, respectively. This is consistent with the effective moment of undoped $FeVO_4$, 5.9 μ_B, being reduced as higher spin Fe^{3+}(s=5/2) is removed from the lattice and replaced with increasing fractions of lower spin Zn^{2+}(s=0), Cr^{3+}(s=3/2) and Mn^{3+}(s=2) transition metal ions as x increases. The Curie-Weiss temperatures (T_θ) also show a drop relative to undoped $FeVO_4$, for which T_θ = 126 K. The Curie-Weiss temperatures are 111 K, 108 K, and 104 K for x=0.05 and 102 K, 93 K, and 92 K at x=0.20 for the Zn, Cr and Mn doped samples respectively. Again, the larger reduction in T_θ for increasing dopant concentrations is consistent with a reduction in the average interaction energy when Fe^{3+} ions are replaced by an increasing fraction of ions having smaller moments.

Since the onset of the multiferroic ordering temperature, T_{N2}, is difficult to determine precisely from magnetic measurements, we used heat capacity measurements for these samples, to probe it more accurately. For these measurements, we mixed $Fe_{1-x}M_xVO_4$ powder samples with Ag powder at 1:1 mass ratio homogeneously and cold-pressed the mixture into a pellet to increase the internal thermal conductivity. We corrected the

measured heat capacity to remove the Ag contribution by subtracting the Ag heat capacity contribution, which was measured separately. Figure 5 plots the heat capacity curves for the Mn, Cr, and Zn doped samples together with that of undoped $FeVO_4$. The curves have been shifted vertically for clarity. There are clear peaks in the heat capacity associated with both the T_{N1} and T_{N2}, allowing for an accurate determination of the transition temperature. Neither the peak intensities nor peak widths show any significant change with chemical doping. The phase transition temperatures for undoped $FeVO_4$ are very consistent with previous studies[20,21], while the doped samples show only a minimal suppression in temperature (Zn and Mn), and even a small increase in transition temperature for Cr doping. We do not see any additional peaks in the doped samples that would indicate either the presence of other phase transitions, or any splitting of the transitions observed in pure $FeVO_4$.

To confirm that T_{N2} still corresponds to the onset of multiferroic order in doped $FeVO_4$, we measured the ferroelectric polarization for selected samples, shown in Fig. 6. For these measurements, the samples were cooled down in a poling field (±200 V) through the transition temperature. This poling field was removed at base temperature and the pyrocurrent was measured while warming at a constant rate of 6 K/min. The ferroelectric polarization was computed by integrating the pyrocurrent with respect to time. Figure 6 shows the ferroelectric polarization for the x=0.05 Cr and Mn doped $FeVO_4$ samples, measured under different applied magnetic fields. The magnitudes of polarization for these x=0.05 samples are 2.6 and 3.1 $\mu C\ m^{-2}$ for Cr and Mn doped $FeVO_4$ respectively, and this polarization is reversible by switching the direction of the poling field. These polarization values are slightly smaller than ~6 $\mu C\ m^{-2}$ for pure $FeVO_4$[21]. This can potentially be attributed to an intrinsic suppression of ferroelectricity in $FeVO_4$ on doping. The polarization shows almost no change when measured under different applied magnetic fields (H = 3, 5 and 7 T), consistent with the very small field dependence observed for the multiferroic phase transition in $FeVO_4$[21]. Moreover, clear reversible polarization is observed to the highest doping fraction (x=0.2) for Zn doped samples[27]. However, as the doping fraction increases, the conductivity of the samples increases, leading to a large leakage current which affects the pyrocurrent measurements. This leads

to a large uncertainty in the magnitude of polarization for samples with > 5% doping. As a result, the magnitude of polarization (1.6 μC m^{-2} as observed for x=0.2 Zn doped $FeVO_4$)[27] may not be reliable. In addition, it was difficult to experimentally obtain the magnitude of ferroelectric polarization for x>0.05 Cr and Mn doped samples due to high leakage current. However, the onset of ferroelectric polarization in type II multiferroics such as $FeVO_4$ arises because of the non-collinear spin structure, breaking the spatial inversion symmetry[22]. Thus, the persistence of the second magnetic phase in these systems after doping, as discussed in magnetic and heat capacity measurements, suggests the possibility of the presence of ferroelectric phase up to the highest doping fraction for Cr and Mn doped samples.

To understand the dependence of the phase transition temperatures on doping, we estimated the transition temperatures, determined from heat capacity measurements, as a function of dopant fraction for $Fe_{1-x}TM_xVO_4$ for both T_{N1} and T_{N2} ferroic ordering. The calculated phase diagram plots are shown in Fig. 7. The relative suppression of the magnetic ordering temperature T_{N1} on Zn and Mn doping is only 2% for the x=0.2 samples, while the multiferroic transition temperature T_{N2} is reduced by only 3% for Mn and 2% for Cr at the same doping fraction. On Cr doping, T_{N1} shows an increase of 1% and T_{N2} shows an increase of nearly 3%. These are remarkably small changes in the magnetic transition temperatures, particularly when compared with results for Zn doped $Ni_3V_2O_8$ which shows a ~30% suppression of the ordering temperature and a ~55% suppression of the multiferroic transition temperature at similar doping fractions[13].

The magnetic transition temperatures in $FeVO_4$ are remarkably insensitive to the presence of either magnetic or non-magnetic dopants, at least up to concentrations of x=0.20. The reduction in the phase transition temperature for $FeVO_4$ cannot be modeled by simple nearest neighbor percolation, which has been shown to be applicable for Zn substituted $Ni_3V_2O_8$[13]. We postulate that the anomalously small decrease in T_{N1} and T_{N2} in $FeVO_4$ on doping may be attributed to a reduction in the geometrical frustration in this system. As shown in Fig. 4, the Curie-Weiss temperature systematically decreases on doping, indicating a reduction in the mean-field magnetic interactions. However, the

magnetic ordering temperature is practically insensitive, the frustration index, defined as T_θ/T_N[28], also decreases, dropping from approximately 6 for pure $FeVO_4$ to 5 for Zn substituted $FeVO_4$ at x=0.20. Motivated by this observation, we suggest that replacing a fraction of Fe^{3+} ions in $FeVO_4$ helps to lift the geometrical frustration and thus, the magnetic ordering temperature is not substantially reduced on doping, even as the mean-field magnetic interaction energy decreases. A similar phenomenon can be observed in the highly frustrated magnet $ZnCr_2O_4$ on doping with Cu. In this system, the transition temperature is practically insensitive to Cu fraction (for x less than approximately 0.30), with T_θ and the frustration index both decreasing monotonically[29]. For $ZnCr_2O_4$ however, unlike $FeVO_4$, the robustness of the ordering temperature seems to depend on the dopant, since Ga doped $ZnCr_2O_4$ exhibits a significant reduction in T_N even for x=0.01[30].

We have studied the effects of transition metal (Zn, Cr, and Mn) dopants on the magnetic phase transitions in $FeVO_4$ using magnetic, dielectric, and thermodynamic measurements. The suppression of the multiferroic ordering temperature and Neel temperature are anomalously small, with the relative suppression being less than 3% for x as large as 0.20 for all dopants. The multiferroic behavior persists up to x=0.20 for Zn, while it is directly experimentally observed only up to x=0.05 for Cr and Mn dopants. However, it is likely that the multiferroic phase persists in Cr and Mn doped samples to the highest doping fraction. The relative stability of the multiferroic phase against doping offers the exciting possibility of using large dopant fractions to tune the magnetoelectric coupling in $FeVO_4$, without eliminating the novel magnetic structures that give rise to ferroelectric ordering.

Acknowledgements

This work was supported by the National Science Foundation through DMR-0644823 and DRM-1306449. We also acknowledge helpful conversations with Ron Baird concerning the analysis of the XRD data.

References:

1 C. Binek and B. Doudin, J. Phy.: Condens. Matter **17** (2), L39 (2005).
2 M. Gajek, M. Bibes, S. Fusil, K. Bouzehouane, J. Fontcuberta, A. Barthelemy, and A. Fert, Nat. Mater. **6** (4), 296 (2007).
3 G. Lawes and G. Srinivasan, J. Phys. D **44** (24), 243001 (2011).
4 L. Zhao, T. L. Hung, C. C. Li, Y. Y. Chen, M. K. Wu, R. K. Kremer, M. G. Banks, A. Simon, M. H. Whangbo, C. Lee, J. S. Kim, I. Kim, and K. H. Kim, Adv. Mater. **24** (18), 2469 (2012).
5 M. Ackermann, D. Brüning, T. Lorenz, P. Becker, and L. Bohatý, New J. of Phys. **15** (12), 123001 (2013).
6 Mandar M. Shirolkar, Changshan Hao, Xiaolei Dong, Ting Guo, Lei Zhang, Ming Li, and Haiqian Wang, Nanoscale **6** (9), 4735 (2014).
7 Z. M. Tian, Y. Qiu, S. L. Yuan, M. S. Wu, S. X. Huo, and H. N. Duan, J. Appl. Phys. **108** (6) (2010).
8 P. Priyadharsini, A. Pradeep, B. Sathyamoorthy, and G. Chandrasekaran, J. Phys. Chem. Solids **75** (7), 797 (2014).
9 C. Nayek, A. Tamilselvan, Ch Thirmal, P. Murugavel, and S. Balakumar, J. Appl. Phys. **115** (7), 073902 (2014).
10 B. Yu, M. Li, J. Liu, D. Guo, L. Pei, and X. Zhao, J. Phy. D **41** (6), 065003 (2008).
11 D. Kothari, V. R. Reddy, A. Gupta, C. Meneghini, and G. Aquilanti, J. Phys.: Condens. Matter **22** (35), 356001 (2010).
12 Y. Du, Z. X. Cheng, X. L. Wang, and S. X. Dou, J. Appl. Phys. **107** (9) (2010).
13 P. Kharel, A. Kumarasiri, A. Dixit, N. Rogado, R. J. Cava, and G. Lawes, Philos. Mag. **89** (22-24), 1923 (2009).
14 A. Kumarasiri and G. Lawes, Phys. Rev. B **84** (6), 064447 (2011).
15 Q. Zhang, W. Knafo, P. Adelmann, P. Schweiss, K. Grube, N. Qureshi, T. Wolf, H. Löhneysen, and C. Meingast, Phys. Rev. B **84** (18), 184429 (2011).
16 L. Meddar, M. Josse, P. Deniard, C. La, G. André, F. Damay, V. Petricek, S. Jobic, M. H. Whangbo, M. Maglione, and C. Payen, Chem. Mater. **21** (21), 5203 (2009).
17 R. P. Chaudhury, F. Ye, J. A. Fernandez-Baca, B. Lorenz, Y. Q. Wang, Y. Y. Sun, H. A. Mook, and C. W. Chu, Phys. Rev. B **83** (1), 014401 (2011).
18 R. P. Chaudhury, B. Lorenz, Y. Q. Wang, Y. Y. Sun, and C. W. Chu, New J. Phys. **11** (3), 033036 (2009).
19 R. P. Chaudhury, F. Ye, J. A. Fernandez-Baca, Y. Q. Wang, Y. Y. Sun, B. Lorenz, H. A. Mook, and C. W. Chu, Phys. Rev. B **82** (18), 184422 (2010).
20 A. Daoud-Aladine, B. Kundys, C. Martin, P. G. Radaelli, P. J. Brown, C. Simon, and L. C. Chapon, Phys. Rev. B **80** (22), 220402 (2009).
21 A Dixit and G Lawes, J. Phys.: Condens. Matter **21** (45), 456003 (2009).
22 A. Dixit, G. Lawes, and A. B. Harris, Phys. Rev. B **82** (2), 024430 (2010).
23 J. Zhang, L. Ma, J. Dai, Y. P. Zhang, Z. He, B. Normand, and W. Yu, Phys. Rev. B **89** (17), 174412 (2014).
24 R. D. Shannon, Acta Crystallogr. Sect. A **32** (5), 751 (1976).
25 P. Schiffer and I. Daruka, Phys. Rev. B **56** (21), 13712 (1997).
26 R. Moessner and A. J. Berlinsky, Phys. Rev. Lett. **83** (16), 3293 (1999).
27 See Supplemental Material at [URL will be inserted by publisher] for x=0.2 Zn polarization measurements.
28 A. P. Ramirez, Annu. Rev. Mat. Sci. **24** (1), 453 (1994).
29 L. Q. Yan, F. Maciá, Z. W. Jiang, J. Shen, L. H. He, and F. W. Wang, J. Phys.: Condens. Matter **20** (25), 255203 (2008).
30 A. D. LaForge, S. H. Pulido, R. J. Cava, B. C. Chan, and A. P. Ramirez, Phys. Rev. Lett. **110** (1), 017203 (2013).

Figures:

Figure 1: Room temperature XRD spectra for (a) Zn, (b) Cr and (c) Mn doped $FeVO_4$ samples.

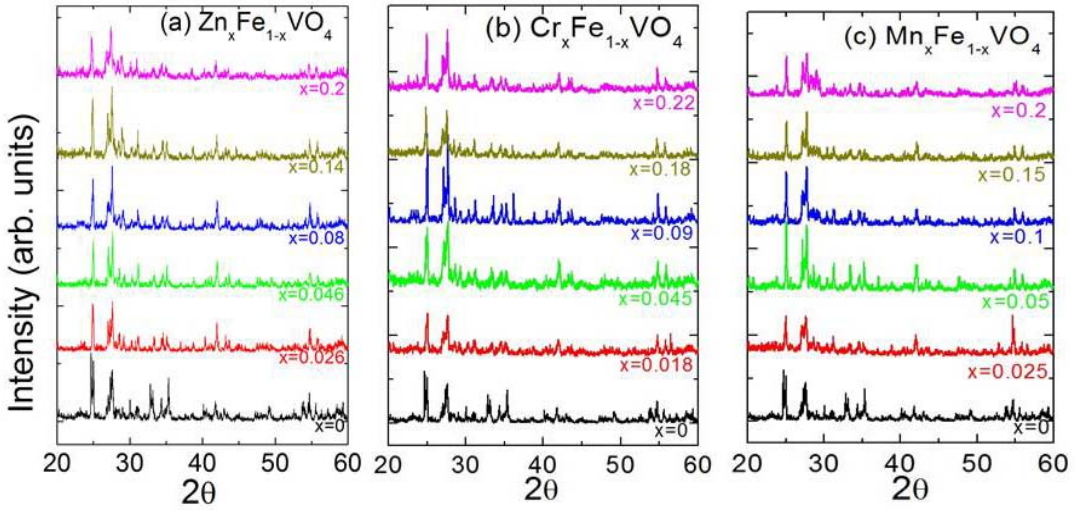

Figure 2: Room temperature Raman spectra for (a) Zn, (b) Cr and (c) Mn doped $FeVO_4$ ($Fe_{1-x}TM_xVO_4$) samples for different x.

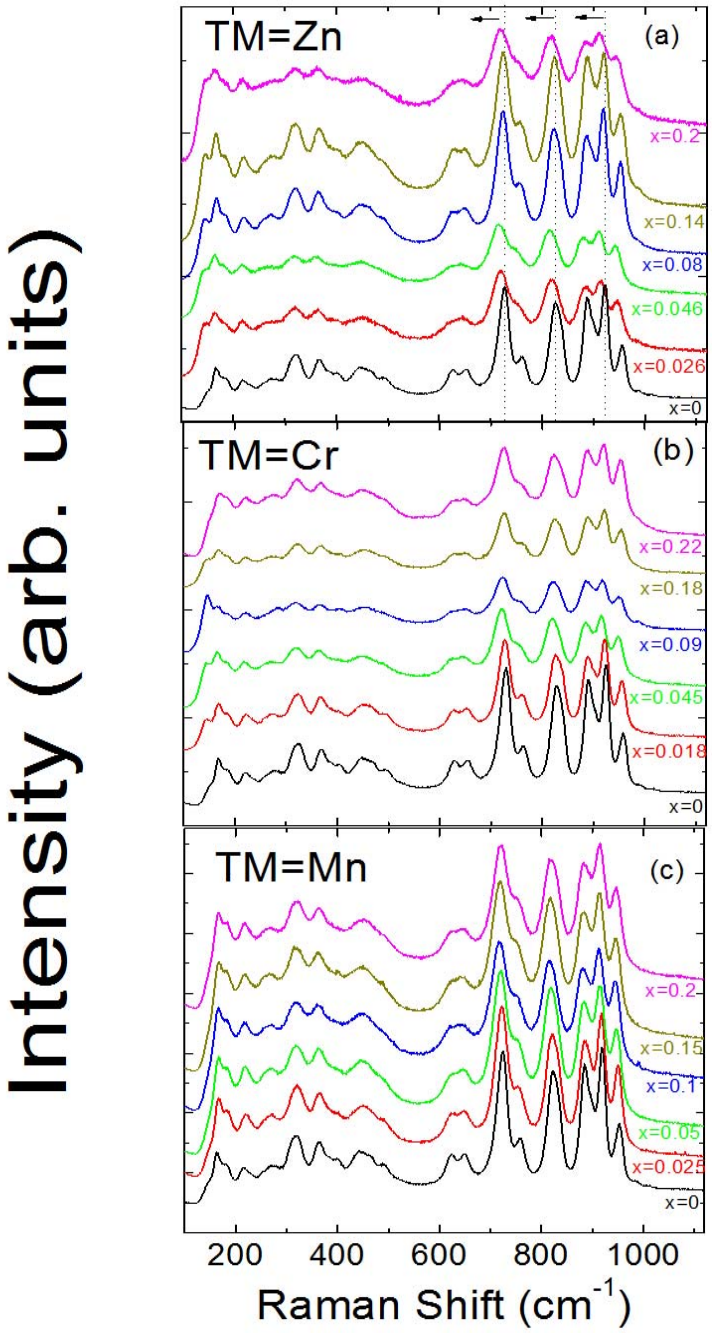

Figure 3: Magnetization versus temperature data for ($Fe_{1-x}TM_xVO_4$), (a) TM=Zn,(b) TM=Cr, (c) TM=Mn samples

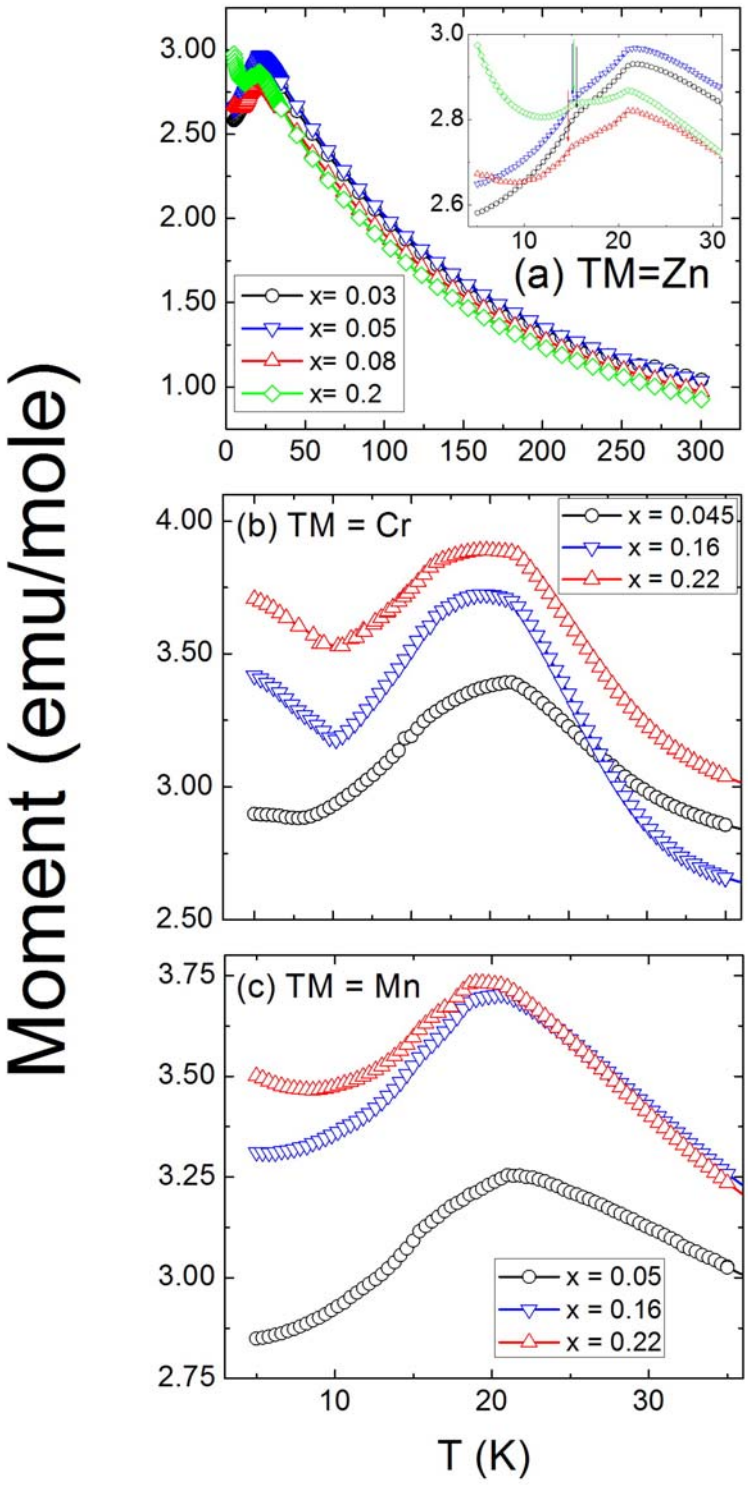

Figure 4: Curie-Weiss fit of the temperature dependent magnetization data with inverse magnetization versus temperature graphs for the $Fe_{1-x}TM_xVO_4$ (a) x=0.05 and (b) x=0.20.

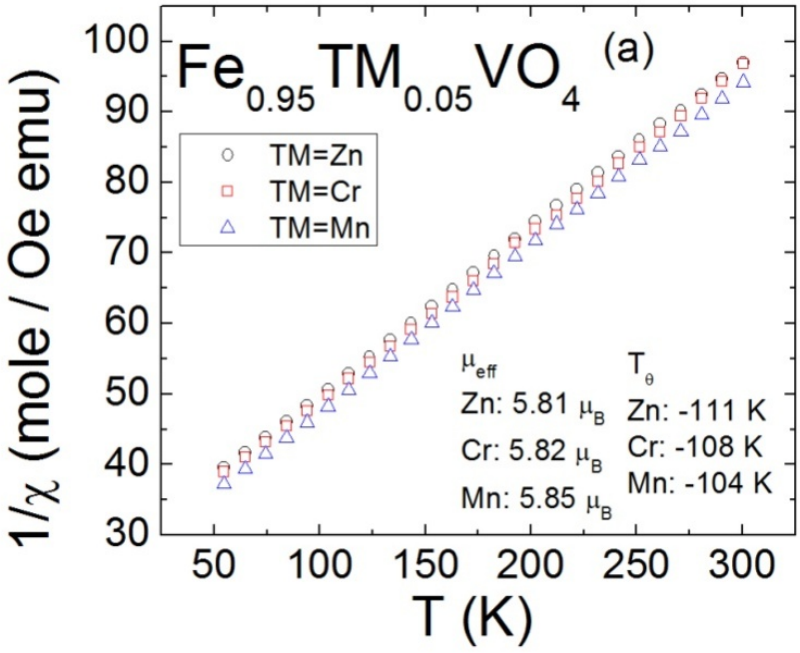

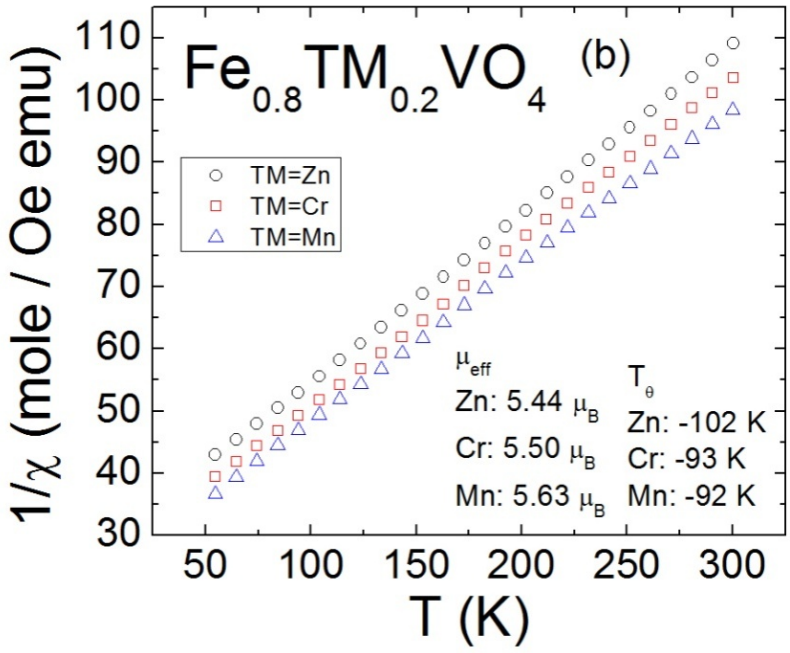

Figure 5: Heat capacity versus temperature curves for the $Fe_{1-x}TM_xVO_4$ samples, where TM = Zn, Cr and Mn.

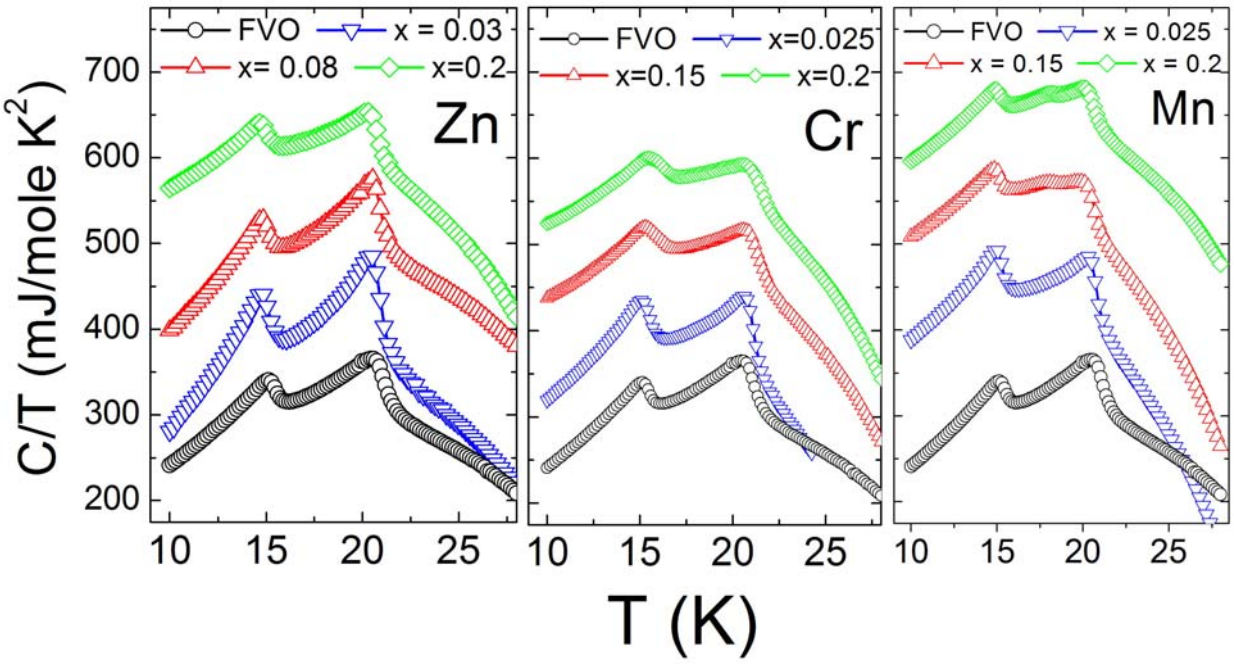

Figure 6: Ferroelectric polarization for x=0.05 Cr and Mn doped $FeVO_4$ samples at different magnetic fields.

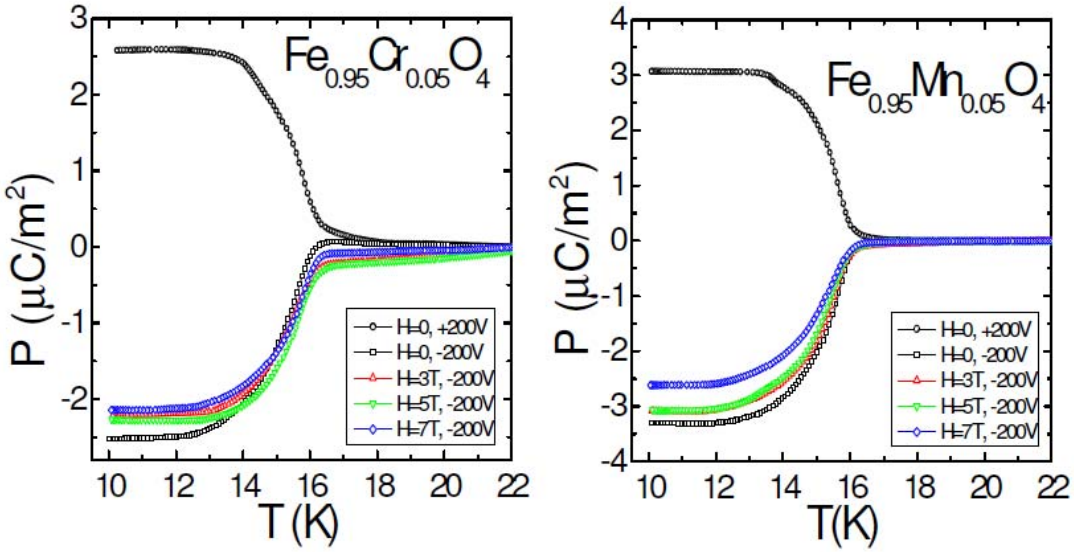

Figure 7: Phase diagrams for the $Fe_{1-x}TM_xVO_4$system; the transition temperature T_{N1} and T_{N2} as a function of the dopant fraction.